การดูดซับแมงกานีสจากน้ำใต้ดินด้วยถ่านชีวภาพยูคาลิปตัส

Manganese Adsorption from Groundwater by Eucalyptus Biochar

อรชพร วิลามาศ[1*] สร้อยดาว วินิจนันทรัตน์[1,2] และ อนวัช พินิจศักดิ์กุล[3]

Arachporn Wilamas[1*] Soydoa Vinitnantharat[1,2] and Anawat Pinisakul[3]

[1]หลักสูตรเทคโนโลยีสิ่งแวดล้อม คณะพลังงานสิ่งแวดล้อมและวัสดุ มหาวิทยาลัยเทคโนโลยีพระจอมเกล้าธนบุรี

[2]กลุ่มวิจัยการจัดการสิ่งแวดล้อมและพลังงานเพื่อชุมชนและเศรษฐกิจหมุนเวียน มหาวิทยาลัยเทคโนโลยีพระจอมเกล้าธนบุรี

[3]หน่วยวิจัยเคมีเพื่อสังคมสีเขียวและสุขภาพ ภาควิชาเคมี คณะวิทยาศาสตร์ มหาวิทยาลัยเทคโนโลยีพระจอมเกล้าธนบุรี

[1]Environmental Technology Program, School of Energy, Environment and Materials,

King Mongkut's University of Technology Thonburi

[2]Environmental and Energy Management for Community and Circular Economy (EEC&C) Research Group,

King Mongkut's University of Technology Thonburi

[3]Chemistry for Green Society and Healthy Research Group (ChGSH), Department of Chemistry, Faculty of Science,

King Mongkut's University of Technology Thonburi

*E-mail: arachaporn.wi@mail.kmutt.ac.th

Received: May 26, 2022

Revised: Jul 20, 2022

Accepted: Jul 26, 2022

บทคัดย่อ

แมงกานีสมักตรวจพบในน้ำใต้ดิน และการดูดซับเป็นวิธีที่นิยมใช้ในการกำจัดแมงกานีส งานวิจัยนี้มีวัตถุประสงค์เพื่อใช้ถ่านชีวภาพยูคาลิปตัสเพื่อดูดซับแมงกานีสจากน้ำใต้ดิน และศึกษาการตรึงโลหะหนักแมงกานีสในถ่านชีวภาพ โดยใช้ถ่านชีวภาพ 1 กรัม ดูดซับน้ำบาดาลที่มีแมงกานีสความเข้มข้น 1.098 มิลลิกรัมต่อลิตร วัดความเข้มข้นของแมงกานีสที่เหลือที่ระยะเวลาต่าง ๆ จนถึงระยะเวลาสมดุล ศึกษาจลนพลศาสตร์ของการดูดซับโดยใช้สมการปฏิกิริยาอันดับหนึ่งเทียมและปฏิกิริยาอันดับสองเทียม นำถ่านชีวภาพที่ดูดซับแมงกานีสแล้วไปสกัดตามลำดับเพื่อหาสัดส่วนรูปของแมงกานีสที่ถูกตรึงในถ่านชีวภาพ เปรียบเทียบกับถ่านชีวภาพที่ยังไม่ได้ใช้ดูดซับ ผลการศึกษาพบว่าถ่านชีวภาพมีความสามารถในการดูดซับแมงกานีสเท่ากับ 0.0146 มิลลิกรัมต่อกรัม ที่ระยะเวลาสมดุล 48 ชั่วโมง และการดูดซับเป็นไปตามปฏิกิริยาอันดับสองเทียม ผลการสกัดตามลำดับพบว่าแมงกานีสถูกตรึงกับส่วนของเหล็กและแมงกานีสออกไซด์สูงที่สุดเป็นสัดส่วนร้อยละ 23.89 ตามด้วยการตรึงในส่วนของสารอินทรีย์ร้อยละ 23.88

คำสำคัญ: ถ่านชีวภาพยูคาลิปตัส การตรึงโลหะ น้ำใต้ดิน การดูดซับแมงกานีส

Abstract

Manganese is frequently detected in groundwater, and adsorption is a popular method for manganese removal. This research aimed to use eucalyptus biochar for manganese adsorption from groundwater and to study the manganese fractionation in the biochar. One gram of eucalyptus biochar was loaded with groundwater containing manganese at the concentration of 1.098 mg/L. Concentrations of the remaining manganese were then measured at different times until reaching the equilibrium time. The pseudo first order and pseudo second order kinetics were applied to examine the adsorption kinetics. Loaded biochars were determined for manganese fractionation by sequential extraction and compared to virgin biochar. The results showed that the biochar had manganese adsorption capacity of 0.0146 mg/g at the equilibrium time of 48 hours. The adsorption kinetic was

followed pseudo second order. The result from the sequential extraction indicated that the highest manganese fraction was bound to iron and manganese oxide at 23.89%, followed by to organic matter at 23.88%.

Keywords: Eucalyptus biochar, Fractionation, Groundwater, Manganese adsorption

1. Introduction

High concentration of manganese (Mn) in groundwater is an environmental issue in Thailand. It was discovered in the northeastern Thailand, such as Ubon Ratchathani province. The Mn concentration was found in ranges of 0.5-2 mg/L. The appearance of black sediment from manganese oxide of stored water can give a fishy odor, produce stains on sanitary ware. Drink of water containing manganese could potentially affect health by toxic accumulation and chronic causes symptoms the brain that controls body movement [1]. Thus, groundwater should be treated before use for safety consumption. Sand and activated carbon filtration is normally used for groundwater treatment in the community. However, activated carbon is expensive causing an increased cost for rural communities. Therefore, the study for using local materials as adsorbents is economically useful. Thus, recently biochar and alternative natural materials was being studied greater and further for heavy metal removal.

Biochar is a carbon rich material which is produced by heating of biomass, or agricultural wastes under limited oxygen. Biochar can be used as a low cost adsorbent for heavy metal removal. For examples poultry manure and farmyard manure-derived biochars were reported as the adsorbents for Mn removal from aqueous solutions [2]; eucalyptus biochar was previously used for removal of cadmium [3] and lead (II) ions [4] from aqueous solutions; eucalyptus-based materials were used as adsorbents for heavy metals and dyes removal from wastewaters [5]; bamboo biochar was successfully used for lead (II) adsorption from solution by Lalhruaitluanga et al [6]. Wang et al. [7] reported that heavy metal contents in chicken manure and water washed swine manure biochar were dependent on pyrolysis temperature. Previous studies [8], [9] reported that use of charcoal was inappropriate for filtering drinking water because various heavy metals found in biochar may be leached out. The chemical fractionation of manganese on the adsorbent material was beneficial for determination of the metal releasing from adsorbents. The forms of Mn fraction are described as dissolution, chemical bonding, binding to organic matter and residual of heavy metals. Thus, the high dissolved and exchangeable fractions could suggest the potential of heavy metal leaching into the environment. Previous studies had examined Mn fractions in soil. Soil amendment with sewage sludge-biochar could reduce Mn mobility in contaminated soils which was attributed to the substantial decrease of the acid-soluble fractions by 70.38% [10]. Woody biochar was reported to be able to immobilize Mn in a serpentine soil by 92% [11]. There are at present only limited data on Mn fractionation in biochar after adsorption in aqueous solution, especially in eucalyptus biochar. Cui et al. [12] studied cadmium and lead fractions in biochar after adsorption and Wang et al. [7] reported heavy metals containing in chicken manure and water-washed swine manure biochars [7].

Eucalyptus is the most widely planted type of hardwood trees. It considers as a cheap, renewable, and ecofriendly biomass source for the production of high value materials. Therefore, it has been an alternative adsorbent to be used for heavy metal removal. Thus, this present study aimed to use eucalyptus biochar for manganese adsorption from groundwater and to study the manganese fractionation in the biochar.

2. Materials and methods

2.1. Groundwater

The groundwater was collected from a residential area in the Warin Chamrap district, Ubon Ratchathani Province. The chemical characteristics of groundwater were shown in Table 1. The total hardness was 420 mg/L as $CaCO_3$. It was classified as very hard [13]. The concentration of initial Mn was 1.098 mg/L which was higher than the maximum allowable concentration (0.5 mg/L) of groundwater for drinking purpose.

Table 1 Characteristics of groundwater in this study

Parameter	Analytical method	Unit	Value
pH	Electrometric Method	-	6.78
Chloride (Cl)	Argentometric Method	mg/L	140
Total Hardness	EDTA Titrimetric Method	mg/L as $CaCO_3$	420
Total Dissolved Solids	Gravimetric Method	mg/L	625
Sulfate (SO_4)	Turbidimetric Method	mg/L	25.28
Nitrate (NO_3)	Colorimetric Method	mg/L	2.99
Iron (Fe)	AAS (Flame)	mg/L	0.174
Manganese (Mn)	AAS (Flame)	mg/L	1.098
Magnesium (Mg)	EDTA Titrimetric Method	mg/L	12.91
Calcium (Ca)	EDTA Titrimetric Method	mg/L	34.75

2.2. Preparation of eucalyptus biochar

Eucalyptus biochar (EB) was used in this study. It was derived from the area in the Warin Chamrap district, Ubon Ratchathani Province. EB was produced using ground pits under oxygen limitation at temperature in the range of 400-500°C [14], [15] and a run was started by introducing eucalyptus branches into the kiln. The process of carbonization started with the burning of auxiliary fuel, such as wood chips, in the top channel of the kiln. The heat from the burning fuel then flowed into the kiln. The kiln was closed by steel cover and clay. When the carbonization occurred, it could be noticed by the smoke released from the chimney. After 6 hours, it was left to cool and the stove was opened. Later, EB was crushed to pieces with sizes in the range of 2-3 mm for using as an adsorbent. The adsorbent was kept in closed containers and used for all experiments.

2.3. Characterization of EB

EB was determined for the external surface structural morphology by scanning electron microscopy (SEM), JEOL Model JSM-7610F Plus, before and after Mn adsorption. The adsorbent surfaces were determined by absorbing the nitrogen gas both onto the surfaces and within the pores of the biochar material by surface area and pore size analyzer (BET- Quantachrome Model Quandrasorb evo). Chemical bonds or functional groups of biochar were analyzed before and after Mn adsorption by Fourier Transform Infrared Spectroscopy techniques (FT-IR), Thermo Scientific Nicolet 6700. Elemental analysis of adsorbent materials using Wavelength Dispersive X–Ray fluorescence Spectrometer (WDXRF), Model Rigaku ZSX Primus. The adsorption capacity of EB was tested according to standard iodine adsorption measurement active standard (ASTM D46070).

2.4. Adsorption equilibration time and kinetics studies

Batch adsorption experiments were carried out to determine the equilibration time of Mn adsorption by EB. The EB dosage of 1 g/20 mL in 30 mL plastic bottle was shaken in the incubator shaker at 100 rpm, 28±0.5°C. Samples were taken at time intervals. The suspensions were filtered through Whatman 42 filter paper at each given time, and the filtrates were analyzed for Mn concentrations by an atomic absorption spectrometer (AAS). The kinetics of Mn adsorption was determined by using two different models: pseudo-first-order kinetic model, and pseudo-second-order kinetic model [16]. The Lagergren pseudo-first-order kinetic model equation is expressed as:

$$q_t = q_e[1 - \exp(-k_1 t)] \quad (1)$$

where

q_e = the amounts of metal ions adsorbed at equilibrium (mg/g)

q_t = the amounts of metal ions adsorbed at time t (mg/g)

k_1 = the Lagergren pseudo-first order adsorption rate constant (min^{-1})

The nonlinear form of the pseudo second-order model can be represented by the equation (2):

$$q_t = \frac{k_2 q_e^2 t}{(1+k_2 q_e t)} \quad (2)$$

where

k_2 = the constant of pseudo second order (g/mg.h)

q_t = the amount of Mn adsorbed at time t (mg/g)

q_e = the amount of Mn adsorbed at equilibrium (mg/g)

The Intra-particle diffusion equation developed by McKay and Poots [17] was used to establish the mechanism of Mn adsorption.

$$q_t = x_i + K' t^{0.5} \quad (3)$$

where

q_t = the amount of Mn adsorbed at time t (mg/g)

x_i = the boundary layer diffusion effects

K' = the rate constant of diffusion, the Mn enters the porosity of the EB ($mg/g.min^{0.5}$)

2.5. Chemical fractionation

To evaluate the distribution pattern of pre and post adsorption of Mn binding on the specific functional groups on biochars, virgin and loaded biochars were used for sequential extraction. Loaded EB biochar was employed by shaking 1 g biochar in 20 mL groundwater for 72 hours. It was found that the remaining Mn concentration in solution was 0.388 mg/L which met the maximum allowable concentration of 0.5 mg/L. A six-step procedure by Tessier et al. [18] was employed with different extractable solvents, as shown in Table 2; water soluble (F1), exchangeable (F2), bound to carbonate (F3), bound to iron and manganese oxide (F4), bound to organic matter and sulfide (F5) and residual (F6).

3. Results and discussion

3.1. EB characteristics

The external surface structural morphology of EB studied by SEM was shown in Figure 1. There were many micropores with diameters ranging from 1 to 10 microns [19]. The amount and size of the pore were temperature dependent [20].

The BET surface area was 152.2 m^2/g, which was higher than other types as shown in Table 3. Biochar had high surface area and pore volumes which had high affinity for metals. Metallic ions could be physically adsorbed onto biochar surface and kept within the pores [21]. The iodine number of EB was 155.42 mg/g, which was higher than rice straw biochar.

The summarized elemental analysis of EB was shown in Table 4. The data of WDXRF revealed that manganese was one of chemical composition in EB (pre adsorption). Then it was increased from 2.11% (pre adsorption) to 4.40% (post adsorption). However, Fe content on EB was decreased after adsorption from 1.53% to 0.57%, due to the fact that iron was readily oxidized and precipitated in the solution.

Table 2 Sequential extraction procedure

Fraction	Type	Extractable Solvent
1	Water soluble	Deionized water
2	Exchangeable	1 M Ammonium acetate, pH 7
3	Bound to carbonate (carbonate)	1 M Ammonium acetate, pH 5
4	Bound to iron and manganese oxide (Fe/MnO)	0.04 M Hydroxylamine hydrochloride in 25% acetic acid (v/v), pH 3
5	Bound to organic matter and sulfide	30% Hydrogen peroxide, 3.2 M Ammonium acetate in 20% HNO_3
6	Residual	7 M HNO_3

Table 3 Characteristics of biochar

Material used for biochar	Pyrolysis temperature (°C)	Iodine No. (mg/g)	Surface area $_{BET}$ (m^2/g)	Pore volume (cc/g)	Pore size (Å)	References
Eucalyptus	400-500	155.42	152.20	0.104	13.37	This study
Poultry manure	450		10.11			[2]
Farmyard manure	450		8.61			[2]
Rice straw	150-400	3.06	14.6	1.690		[20]
Switchgrass	300		2.90		50.02	[21]
Swine manure*	550		17.07	0.058	1.896	[22]

*Surface-modified biochar

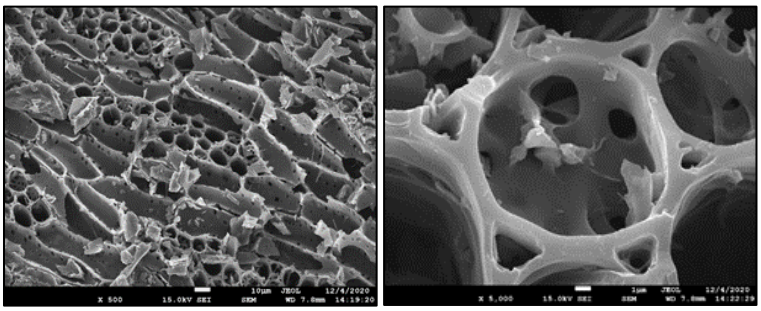

A B

Figure 1 SEM images of external surface structural morphology of EB: (A) 500x; (B) 5000x

Table 4 Summarized elemental analysis of adsorbent material by WDXRF

Element	% Weight	
	Pre adsorption	Post adsorption
P	2.67	1.79
K	27.60	18.30
Ca	50.4	60.80
Mn	2.11	4.40
S	1.06	0.73
Si	7.11	6.58
Fe	1.53	0.57
Al	0.48	0.19
Cl	2.90	0.96
Zn	0.26	0.33
Mg	3.80	5.26
Cu	0.12	0.15

The FTIR spectra of pre and post Mn adsorption on the adsorbents were recorded between 400 and 4000 cm^{-1} by spectrometer as shown in Figure 2. The characteristic bands intensive peaks appeared in the 3500–3400 cm^{-1} corresponding to the O-H stretching. There was another peak observed at 1617 cm^{-1} corresponding to the C=C stretching that could be attributed to the presence of aromatic or benzene rings [23]. A relatively small peak was found at 1381 cm^{-1} for C-H biochar indicative of lignin. Meanwhile, the characteristic peaks in 617-597 cm^{-1} associated with Mn-O vibrations were detected [24], [25].

For the FTIR spectra of post Mn adsorption, the -OH band in EB shifted towards Mn adsorbed EB suggesting Mn^{2+} binding with OH^- group. According to previous report, EB had negatively charged surfaces (COO and OH^-) for Pb^{2+} attraction [26].

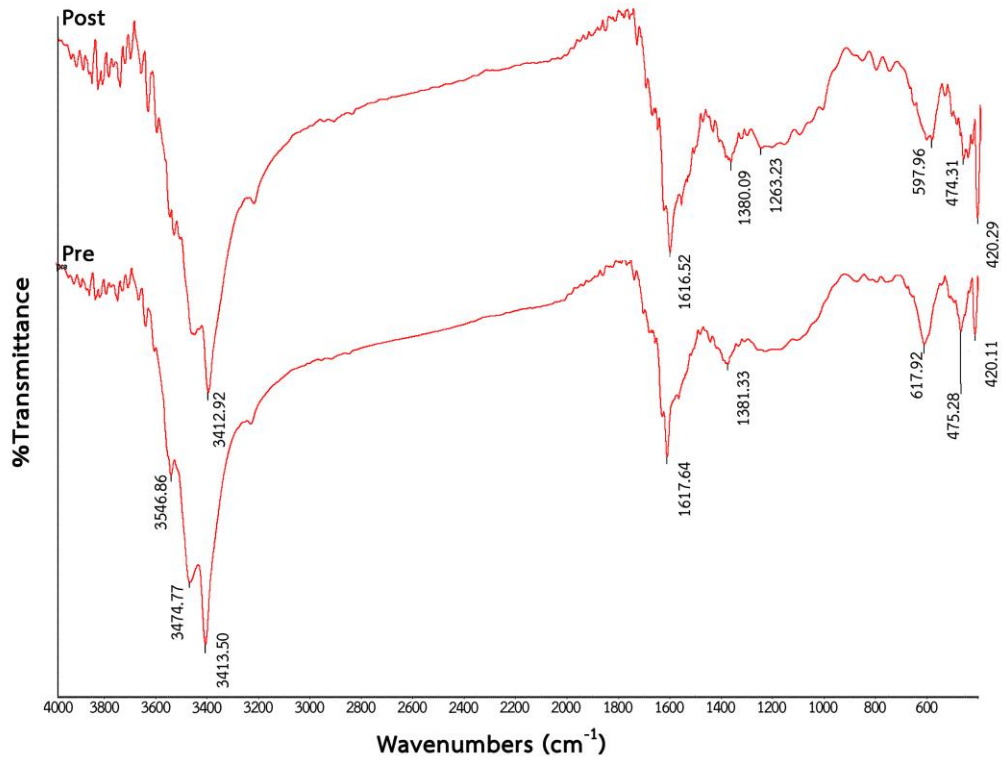

Figure 2 FTIR spectra of pre and post Mn adsorption on the adsorbents (EB)

3.2. Effect of contact time

The Mn adsorption capacity (mg/g) at different times was shown in Figure 3. The adsorption occurred rapidly before 24 hours, then was slow down and stable at 48 hours. It was observed that EB had maximum Mn adsorption capacity of 0.0146 mg/g. To ensure the batch adsorption reached the equilibrium of adsorption and desorption, the contact time of 72 hours was selected.

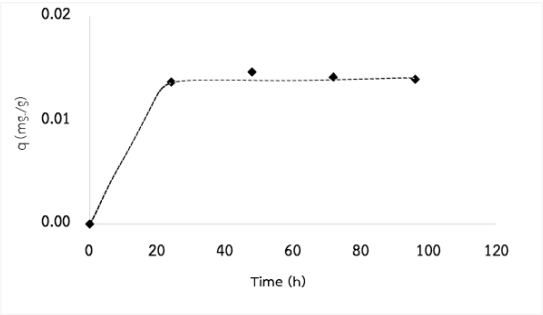

Figure 3 Effect of contact time on the Mn adsorption

3.3. Adsorption kinetics

Pseudo-first order and pseudo-second order kinetic models were applied to interpret the mechanisms of Mn adsorption onto EB surfaces. The kinetic parameters from this study were shown in Table 5. It could be concluded that Mn adsorption followed the pseudo-second-order model with the correlation coefficient R^2 greater than 0.9985. In addition, the amount of Mn adsorbed from experiment (q_{exp}) was close to the amount of Mn adsorbed from model (q_e). This indicated the rate-limiting step was a chemical adsorption through valence force sharing or exchange of electrons between EB and Mn^{2+} [27], correlating to Mn binding to the O-H group of EB surface. In Table 5, the regression of metal ions (0.7794) showed the existence of intra-particle diffusion mechanism on the sorption of Mn ions onto EB Initially. The adsorption was immediate, while the second stage was the adsorption equilibrium, with the K' of 0.0002 mg/g.$min^{0.5}$. It led to a slower diffusion rate of Mn into the absorbent material, compared to the absorption of Mn (II) ions from aqueous solution onto a Nigerian kaolinite clay [28] which had a faster diffusion rate in the sorbent with the K' of 2.75 mg/g.$min^{0.5}$.

Table 5 Adsorption kinetic parameters

PFO	q_{exp} (mg/g)	0.0146
	k_1 (h^{-1})	0.029
	q_e (mg/g)	0.000135
	R^2	0.114
PSO	q_{exp} (mg/g)	0.0146
	k_2 (g/mg.h)	3.067
	q_e (mg/g)	0.0140
	R^2	0.9985
Intraparticle diffusion	K' (mg/g.$min^{0.5}$)	0.0002
	R^2	0.7794

3.4. Chemical fractionation

The percentage of Mn fractions in biochar from the sequential extraction of pre and post Mn adsorption of EB was shown in Figure 4. High percent content of Mn in virgin EB was bound to residue (F6) and followed by organic matter (F5) with the values of 32.35 and 27.93%, respectively. Mn fractions of loaded EB shifted to iron binding and manganese oxide binding (F4) at 23.89, corresponding to the binding with OH group and 23.88% with organic matter. It could be described that the binding of Mn onto iron and manganese oxide was strong. Mn could be adsorbed on the EB surface efficiently, and conformity with chemical adsorption corresponded to the pseudo-second order kinetic data. The summation of Mn fraction in F1, F2 and F3 was 32.27% of total Mn fractions, showing that Mn might be desorbed from loaded biochar [29].

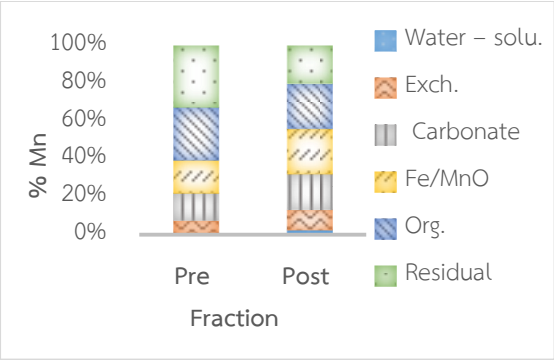

Figure 4 Chemical fractionation of eucalyptus biochar

4. Conclusion

EB had maximum Mn adsorption capacity of 0.0146 mg/g at pH of 6.7±0.1, and at 48 h, for equilibrium time. The kinetic study showed that the pseudo-second-order model was more described by the Mn removal from groundwater. The Mn concentration using sequential extraction showed that the manganese in iron-binding and manganese oxide was strong. Supportive capacity binding with manganese oxide pointed out the conformity with chemical adsorption accepted the pseudo-second-order kinetic data records. The amount of EB at 1 g/20 mL was effective for Mn removal through the adsorption process.

5. Acknowledgements

The authors are grateful to the School of Energy, Environment and Materials, King Mongkut's University of Technology Thonburi for partial financial support, and to the Faculty of Science, Ubon Ratchathani University for providing a laboratory to conduct research.

6. References

[1] Schneider, J.S. and et al. 2013. Chronic manganese exposure impairs visuospatial associative learning in non-human primates. **Toxicology letters.** 221(2): 146-151.

[2] Idrees, M. and et al. 2018. Adsorption and thermodynamic mechanisms of manganese removal from aqueous media by biowaste-derived biochars. **Journal of Molecular Liquids.** 266: 373-380.

[3] Venkatesan, G., Senthilnathan, U. and Rajam, S. 2014. Cadmium removal from aqueous solutions using hybrid eucalyptus wood based activated carbon: Adsorption batch studies. **Clean Technologies and Environmental Policy.** 16(1): 195-200.

[4] Singh, B., Walia, B.S. and Arora, R. 2018. Eucalyptus wood charcoal as Biosorbent for removal of lead (II) ions from aqueous solution. **International Journal of Research and Analytical Reviews.** 5(4): 933-938.

[5] Anastopoulos, I., Ahmed, M.J. and Hummadi, E.H. 2022. Eucalyptus-based materials as adsorbents for heavy metals and dyes removal from (waste)waters. **Journal of Molecular Liquids.** 356: 118864.

[6] Lalhruaitluanga, H. and et al. 2010. Lead (II) adsorption from aqueous solutions by raw and activated charcoals of *Melocanna baccifera* Roxburgh (bamboo) - A comparative study. **Journal of Hazardous Materials.** 175(1-3): 311-318.

[7] Wang, A. and et al. 2021. Speciation and environmental risk of heavy metals in biochars produced by pyrolysis of chicken manure and water-washed swine manure. **Scientific Reports.** 11(1): 1-14.

[8] Mancinelli, E. and et al. 2016. Trace metals in biochars from biodegradable by-products of industrial processes. **Water, Air & Soil Pollution.** 227(6): 1-21.

[9] Zhou, Z.F. 2015. Content of heavy metals in BioChars and assessment of ecological risk on their application to soil. In: **Proceedings of the International Conference on Energy, Environmental & Sustainable Ecosystem Development,** 21-23 August 2015. Kunming, China.

[10] Zhou, D. and et al. 2017. Effects of biochar-derived sewage sludge on heavy metal adsorption and immobilization in soils. **International Journal of Environmental Research and Public Health.** 14(7): 681.

[11] Bandara, T. and et al. 2017. Efficacy of woody biomass and biochar for alleviating heavy metal bioavailability in serpentine soil. **Environmental Geochemistry and Health.** 39(2): 391-401.

[12] Cui, L. and et al. 2015. Does biochar alter the speciation of Cd and Pb in aqueous solution. **Bioresources.** 10(1): 88-104.

[13] Saha, S., Reza, A.S. and Roy, M.K. 2019. Hydrochemical evaluation of groundwater quality of the Tista floodplain, Rangpur Bangladesh. **Applied Water Science.** 9: 198.

[14] Burnette, R. 2016. **Charcoal Production in 200-Liter Horizontal Drum Kilns.** https://www.echocommunity.org/resources/069529b4-0ce4-475c-99b8-326957e3afa7. Accessed 1 July 2022.

[15] Tippayawong, N. and et al. 2010. Production of charcoal from woods and bamboo in a small natural draft carbonizer. **International Journal of Energy Environmental.** 1(5): 911-918.

[16] Ho, Y.S. and McKay, G. 1998. Kinetic models for the sorption of dye from aqueous solution by wood. **Process Safety and Environmental Protection.** 76(2): 183-191.

[17] Mckay, G. and Poots, V.J. 1980. Kinetics and diffusion processes in colour removal from effluent using wood as an adsorbent. **Journal of Chemical Technology & Biotechnology.** 30: 279-292.

[18] Tessier, A.P.G.C., Campbell, P.G. and Bisson, M.J.A.C. 1979. Sequential extraction procedure for the speciation of particulate trace metals. **Analytical Chemistry.** 51(7): 844-851.

[19] Mukherjee, A., Zimmerman, A.R. and Harris, W. 2011. Surface chemistry variations among a series of laboratory-produced biochars. **Geoderma.** 163: 247-255.

[20] Khawkomol, S. and et al. 2021. Potential of biochar derived from agricultural residues for sustainable management. **Sustainability.** 13(15): 814.

[21] Kumar, S. and et al. 2011. An assessment of U (VI) removal from groundwater using biochar produced from hydrothermal carbonization. **Journal of Environmental Management.** 92(10): 2504-2512.

[22] Jiang, B., Lin, Y. and Mbog, J.C. 2018. Biochar derived from swine manure digestate and applied on the removals of heavy metals and antibiotics. **Bioresource Technology.** 270: 603-611.

[23] Koseoglu, E. and Akmil-Basar, C. 2015. Preparation, structural evaluation and adsorptive properties of activated carbon from agricultural waste biomass. **Advanced Powder Technology.** 26(3): 811-818.

[24] Ding, Y. and et al. 2020. Mesoporous MnO 2/SBA-15 as a synergetic adsorbent for enhanced uranium adsorption. **New Journal of Chemistry.** 44(32): 13707-13715.

[25] Yang, C. and et al. 2020. The preparation of a novel iron/manganese binary oxide for the efficient removal of hexavalent chromium [Cr (vi)] from aqueous solutions. **RSC Advances.** 10(18): 10612-10623.

[26] Mohair, D. and Pittman, C.U. 2007. Arsenic removal from water/wastewater using adsorbents - A critical review. **Journal of Hazardous Materials.** 142(1-2): 1-53.

[27] Ho, Y.S. and McKay, G. 1999. Pseudo-second order model for sorption processes. **Process Biochemistry.** 34(5): 451-465.

[28] Dawodu, F.A. and Akpomie, K.G. 2014. Simultaneous adsorption of Ni(II) and Mn(II) ions from aqueous solution unto a Nigerian kaolinite clay. **Journal of Materials Research and Technology.** 3(2): 129-141.

[29] Nkinahamira, F. and et al. 2019. Occurrence, geochemical fractionation, and environmental risk assessment of major and trace elements in sewage sludge. **Journal of Environmental Management.** 249: 109427.